ACSNANO

www.acsnano.org

ARTICLE

Biomechanical Energy Harvesters Based on Ionic Conductive Organohydrogels via the Hofmeister Effect and Electrostatic Interaction

Yinghong Wu, Jingkui Qu, Xinghan Zhang, Kelong AO, Zhiwen Zhou, Zeyang Zheng, Yijie Mu, Xinya Wu, Yang Luo,* and Shien-Ping Feng*

Cite This: https://doi.org/10.1021/acsnano.1c03830

ABSTRACT: The recent use of cryoprotectant replacement method for solving the easy drying problem of hydrogels has attracted increasing research interest. However, the conductivity decrease of organohydrogels due to the induced insulating solvent limited their electronic applications. Herein, we introduce the Hofmeister effect and electrostatic interaction to generate hydrogen and sodium bonds in the hydrogel. Combined with its double network, an effective charge channel that will not be affected by the solvent replacement, is therefore built. The developed organohydrogel-based single-electrode triboelectric nanogenerator (OHS-TENG) shows low conductivity decrease (one order) and high output (1.02−1.81 W/m^2), which is much better than reported OHS-TENGs (2−3 orders, 41.2−710 mW/m^2). Moreover, replacing water with glycerol in the hydrogel enables the device to exhibit excellent long-term stability (four months) and temperature tolerance (−50−100 °C). The presented strategy and mechanism can be extended to common organohydrogel systems aiming at high performance in electronic applications.

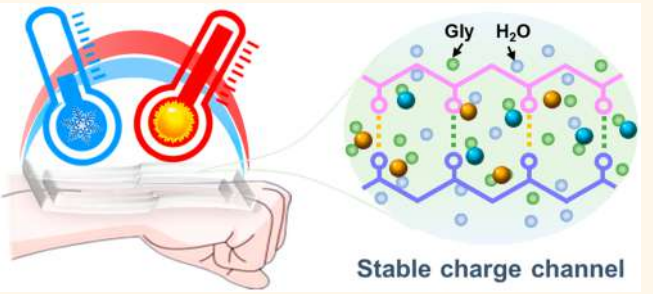

KEYWORDS: *energy harvesting, triboelectric effect, ionic conductive organohydrogel, Hofmeister effect, electrostatic interaction, wearable applications*

The rapid progress of next-generation wearable electronics has driven increasing demands for power sources with flexibility, stretchability, and sustainability.[1−3] However, the common used power suppliers, such as batteries and supercapacitors, are limited by their rigid structure, complex fabrication, and non self-charging ability. Thanks to the advent of flexible nanogenerators that convert ambient mechanical energy into electricity, the soft and sustainable power sources have been well developed in recent years.[4−7] In virtue of its high output, lightweight, and low cost, flexible triboelectric nanogenerator (TENG) based on coupling effect of contact electrification and electrostatic induction is considered as one of the most promising wearable power sources for human motion energy harvesting.[8−10] In particular, the single-electrode TENG (S-TENG) using hydrogel as the ionic conductor has gained increasing attention because of its merits of conductivity, stretchability, and transparency.[11]

However, the main hurdle of hydrogel-based S-TENG (HS-TENG) is its easy-to-dry property, which leads to a narrow operating temperature window and short life span. Although several recent studies have reported that their HS-TENGs can maintain a stable output in the temperature range of 0−60 °C[12,13] or −20−25.8 °C,[14] the introduction of salts or chemicals cannot inhibit but only retard the water evaporation, and thus the resulting devices in these studies can only keep their stable output in 20−30 days storage. Recently, ionic liquid has been introduced in the HS-TENG to widen the working temperature range to −20−100 °C, but cost and toxicity to human and the environment are a concern.[15] Hence, there is an urgent need for a cost-effective and environmentally friendly method to fabricate HS-TENGs with excellent temperature-tolerance and long-term output stability.

In 2018, Chen et al. synthesized an anti-freezing and nondrying organohydrogel via one-pot solvent displacement, where the as-prepared hydrogel was immersed in the

Received: May 6, 2021
Accepted: August 4, 2021

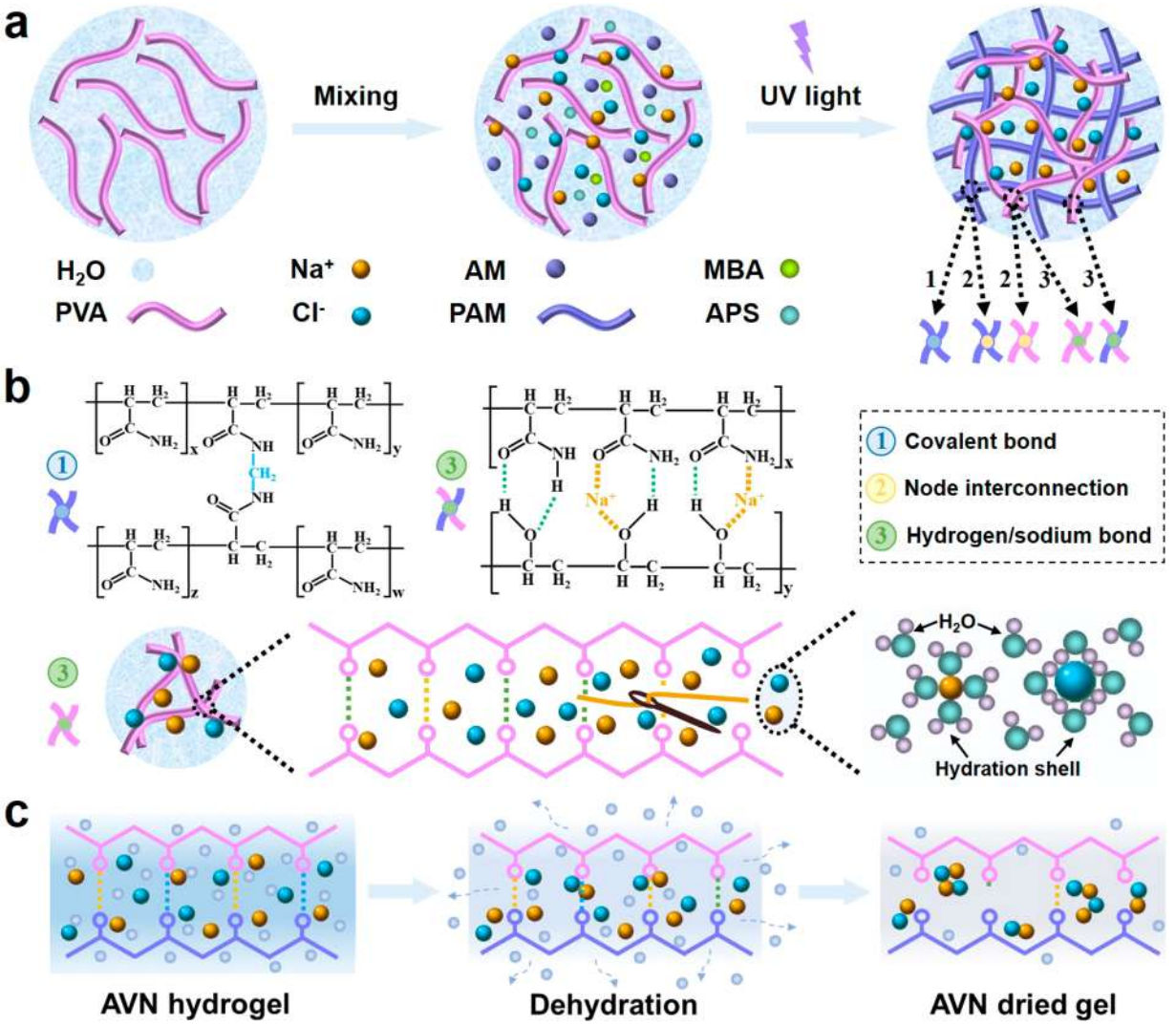

Figure 1. Schematic illustration of AVN hydrogels: (a) synthesis process, (b) generated chains and bonds where NaCl works as a needle and thread to sew the PAM and PVA polymers by forming hydrogen bonds and sodium bonds with stronger bond strength among polymers via the salting-out effect and electrostatic interaction, respectively, and (c) dehydration process.

cryoprotectant to replace water.[16] Inspired by this method, Huang et al.[17] recently replaced partial water of PAM/Clay hydrogels with glycerol and further developed an organohydrogel-based S-TENG (OHS-TENG) that shows good temperature tolerance (−30−80 °C). However, a nonignorable shortcoming of this method is the low conductivity the organohydrogel due to the loss of water molecules and the introduction of insulated glycerol. Although Sun et al.[18] have considered carbon nanotubes (CNTs) as conductive additives and montmorillonite (MMT) as dispersants in polyacrylamide (PAM) hydrogels. The conductivity of PAM/MMT/CNT hydrogels still decreased from 10^{-4} S/cm to $10^{-6} \sim 10^{-7}$ S/cm after glycerol replacement, leading to the power density of its resulting OHS-TENG only achieved 41.2 mW/m^2. Thus, more effective strategies are needed to develop conductive organohydrogels for OHS-TENGs with high output.

Herein, we present a sustainable ionic conductive OHS-TENG with high output and excellent environmental tolerance via the Hofmeister effect and electrostatic interaction. The reported works mainly focused on the mechanical properties and output enhancement of HS-TENGs; this work has studied the internal mechanism of the formed hydrogen bonds and sodium bonds among polymer networks. Besides, the reported OHS-TENGs paid much attention to the physical properties (such as nondrying and anti-freezing properties) of the organohydrogels, we focus more on the insight of ions transfer and bonds change during the solvent replacement process. With an effective charge channel, the conductivity (1.03−5.93 × 10^{-5} S/cm) and power density (1.02−1.81 W/m^2) of the resulting OHS-TENG is much higher than the reported OHS-TENGs ($10^{-6} \sim 10^{-7}$ S/cm, 41.2−710 mW/m^2). Besides, the developed device exhibited ultralong-term output stability (>4 months) under ambient conditions and excellent temperature tolerance (−50−100 °C) via a real-time temperature-output monitoring system. Finally, we demonstrated the wearable applications, that is, when the OHS-TENG device was in contact with skin or clothes, the generated electricity can directly light up LEDs, monitor human's motion, or be stored to drive commercial electronics.

RESULTS AND DISCUSSION

As shown in Figure 1a, the PAM/PVA/NaCl (AVN; [PVA represents poly(vinyl alcohol)]) hydrogel was synthesized by a simple one-pot method with the assistance of UV light. For

https://doi.org/10.1021/acsnano.1c03830
ACS Nano XXXX, XXX, XXX−XXX

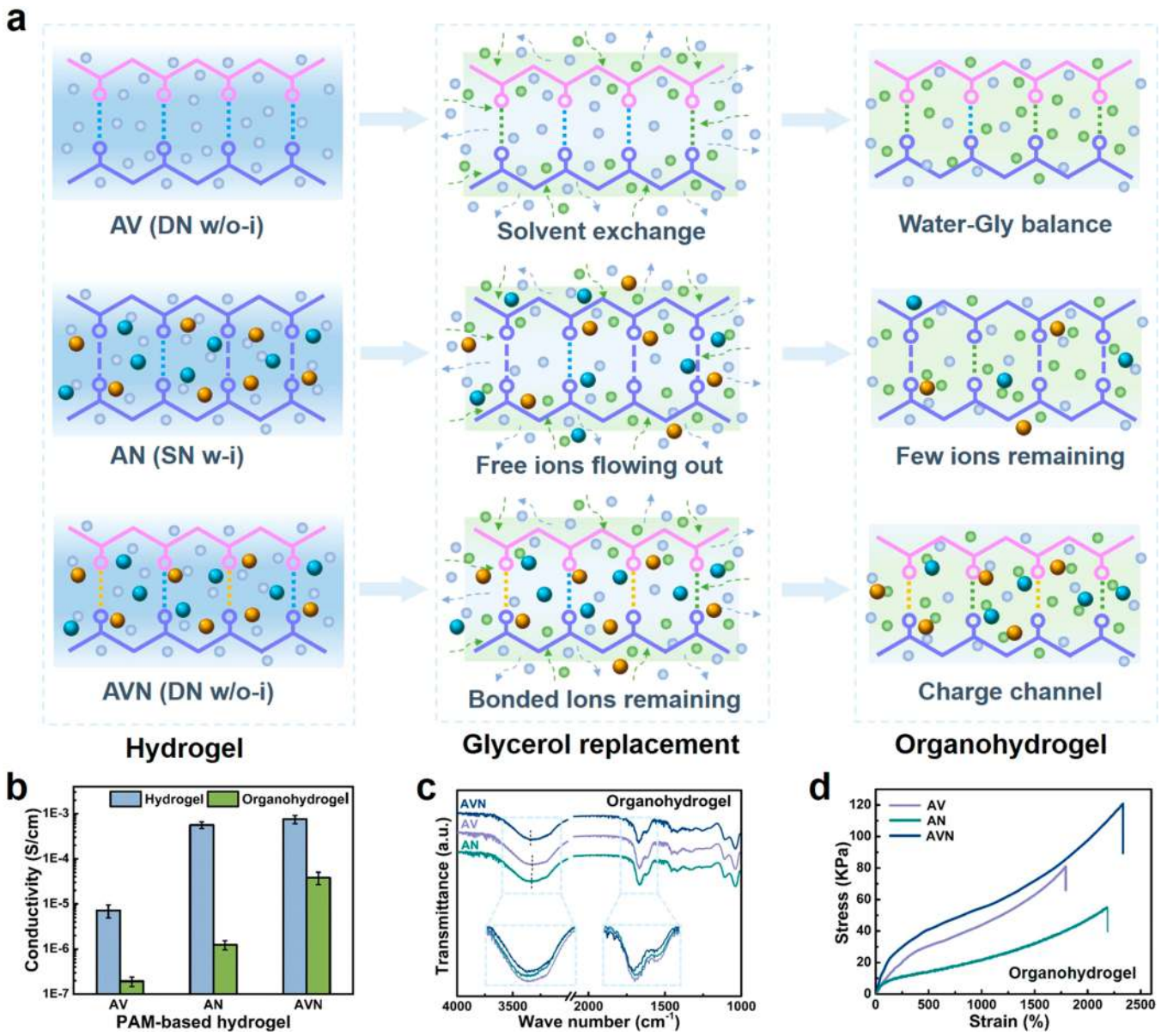

Figure 2. Solvent replacement mechanism and physical properties: (a) Schematic mechanism of solvent replacement process via the Hofmeister effect and electrostatic interaction for different hydrogels, (b) conductivity of different hydrogels before and after solvent replacement, (c) FTIR spectra and (d) stress−strain curves of different organohydrogels.

comparison, PAM/NaCl (AN) and PAM/PVA (AV) hydrogels were prepared with the same procedure. The tough network in AVN hydrogel is obtained based on the covalent bonds formed in PAM, the node interconnections between PAM and PVA, as well as the generated hydrogen and sodium bonds (Figure 1b), which can be verified by the FTIR results. As shown in Supporting Information (SI) Figure S1, the addition of NaCl in PAM and AV hydrogels leads to the −OH stretching peak shifts from 3360−3368 cm^{-1} to 3385−3395 cm^{-1}, indicating the formation of intermolecular hydrogen bonds in AN and AVN hydrogels due to the salting-out of polymers based on the Hofmeister effect.[11,19] Besides, compared to the other three hydrogels, the obviously reduced peak intensity of carbonyl (right) and hydroxy (left) in AVN hydrogel, as seen in the inset of SI Figure S1, implying the generation of stronger sodium bonds via electrostatic interaction.[20,21] Moreover, the generated hydration shells among Na and Cl ions help them to evenly separate in the hydrogels and build a conductive charge channel with generated bonds and chains over the whole system. However, the water evaporation during the dehydration process breaks these hydration shells and bonds, leading to the aggregation of Na and Cl ions inside the hydrogel (Figure 1c) and eventually the loss of conductivity in the AVN dried gel.

In order to solve this problem, the as-prepared hydrogels were immersed in the glycerol solution, and the water molecules in the hydrogel therefore will be displaced by the surrounding glycerol molecules.[16,22] Different from Wu et al.'s researches that have directly considered organohydrogels as the strain/temperature sensors to monitor human motion/heat,[23−25] the developed organohydrogels in this work is considered as the flexible electrode of the S-TENG. To further explain the inhibiting mechanism of the conductive charge channel inside AVN hydrogel on the conductivity decrease

https://doi.org/10.1021/acsnano.1c03830
ACS Nano XXXX, XXX, XXX−XXX

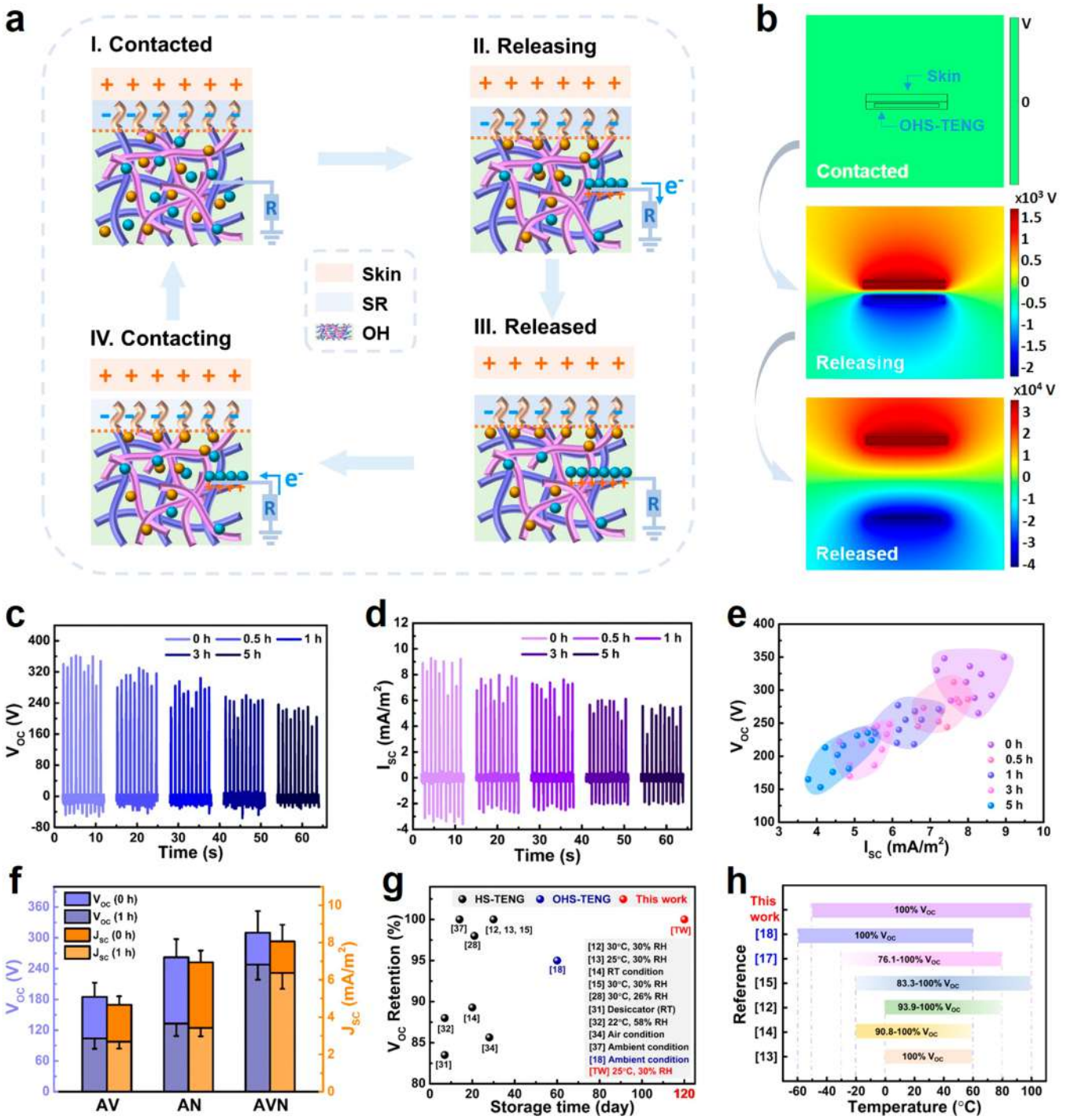

Figure 3. Working mechanism and output performance of AVN-based OHS-TENG: (a) working principle of the AVN-based OHS-TENG when considering skin as the positive material, (b) simulation results of the electrical potential distribution at contacted, releasing and released states, (c) V_{OC}, (d) J_{SC}, (e) repeatability (10 devices for each condition) and (f) output of various devices before and after 1-h glycerol immersion, and (g) output stability and (h) temperature tolerance compared with reported works.

during the glycerol replacement, the conductive principles of AV and AN hydrogels are also studied. It is noted that AV, AN, and AVN hydrogels in this work represent common hydrogels with double network but no free ions (DN w/o-i), single network with free ions (SN w-i), and double network with free ions (DN w-i), respectively. The solvent replacement process for these three systems is schematically illustrated in Figure 2a, which could be explained together with the physical properties presented in Figure 2b–d.

Although the conductivity in Figure 2b shows decrease trend for all organohydrogels after glycerol replacement, the decrease order and reasons of these hydrogels vary a lot. For AV hydrogels (DN w/o-i), the main factor comes from partial hydrogen bonds formed from water molecules replaced by those from glycerol molecules. Thus, its conductivity decreased from a relatively low level (10^{-6} S/cm) to an even lower level (10^{-7} S/cm) after the system achieved a water-glycerol balance. While for AN (SN w-i) and AVN (DN w-i)

https://doi.org/10.1021/acsnano.1c03830
ACS Nano XXXX, XXX, XXX−XXX

hydrogels, the situations are much more complicated. As illustrated in Figure 2a, there are many free Na and Cl ions existing in both hydrogels, leading to their similarly high conductivity (5.60−7.56 × 10^{-4} S/cm, Figure 2b). However, the conductivity of the AN system dramatically dropped by two orders (1.24 × 10^{-6} S/cm) after glycerol replacement, which is 30 times lower than the AVN organohydrogel (3.84 × 10^{-5} S/cm) under the same procedure. There are two main factors ascribing to this phenomenon. One is the polymer networks. Compared to the AN hydrogel with a single network, the double network of the AVN hydrogel confirmed by the SEM images in SI Figure S2, is able to "bond" more Na and Cl ions on the polymer chains through dipole interactions.[26,27] Therefore, there are more ions existing in the AVN system but less in AN system after glycerol replacement as schematic in Figure 2a. The other factor is the generated bonds. According to the FTIR results of these organohydrogels (Figure 2b), sodium bonds generated via electrostatic interaction are still found in AVN organohydrogel, indicating the replacement of water with glycerol hardly breaks the sodium bonds that are much stronger than hydrogen bonds. Therefore, combining the bonded ions and sodium bonds with the regenerated hydrogen bonds, the conductive channel remaining in the AVN organohydrogel is responsible for its high conductivity, which is comparable to reported hydrogels presenting excellent conductivity without insulated solvent replacement.[14,28] More supporting analysis based on Raman and ICP-OES data (Figure S3 and Table S1) can be found in the Supporting Information.

It is noted that the conductivities of reported PEGDA organohydrogel fiber (7.65 × 10^{-3} S/cm)[29] and KI salt-glycerol solution (7.4 Ω/m = 1.35 × 10^{-3} S/cm)[30] are higher than the developed AVN organohydrogel in this work. It is mainly because the organohydrogel fiber was soaked in a glycerin:water (1:1) solution with 0.5 M KCl and 0.023 M $CaCl_2$, while the salt-glycerol solution was obtained by directly dissolving KI in the glycerol. However, the situation of our work is quite different, in which the hydrogel was soaked in a pure glycerol solution to maximize the effect of sodium and hydrogen bonds but minimize the potential effect of remaining NaCl on the conductivity and performance of the organohydrogel. This leads to excessive NaCl overflow during the solvent replacement process and further reduces the conductivity of the organohydrogel system.

Furthermore, the tensile strength and elongation at break of AVN organohydrogel in Figure 2d reached 120.7 KPa and 2333%, respectively, which are higher than 81.1 KPa and 1792% of the AV hydrogel and 55.1 KPa and 2186% of the AN hydrogel. This indicates that the coupling effect of stable bonds and double network structures also contributes to the mechanical properties improvement of hydrogels, benefiting its use in stretchable and flexible wearable electronics. In this case, the TENG using AVN organohydrogel as the electrode and silicone rubber (SR) as the triboelectric layer, was fabricated based on the procedure described in SI Figure S4. SI Figure S5 shows the photograph of a typical AVN-based OHS-TENG, where the device can stand extremely rolling, twisting and stretching (SI Figure S6a as well), as the packaging SR also shows excellent flexibility and durability (SI Figure S6b). Besides, the transparency of the AVN organohydrogel and OHS-TENG can achieve ∼87% and ∼75% in the visible light range (SI Figure S7), respectively, which endows visual information transmission for the electronic skin.

Moreover, the anti-drying and anti-freezing properties of both AVN-based organohydrogels and their corresponding TENGs were systematically studied in SI Figure S8 and SI Figure S9. It is concluded that, compared to those without glycerol immersion drying out in 1−2 weeks (25 °C, 30% RH) and freezing in 1 day (−20 or −50 °C), AVN organohydrogels and its resulting OHS-TENGs with glycerol soaking can maintain their weight, flexibility and transparency, even after four months of storage under the same conditions. To the best of our knowledge, our device exhibited exceptional long-term stability in both ambient and harsh environment, outperforming all the reported HS-TENGs and OHS-TENGs.[12−15,17,18,28,31−34] Detailed discussion concerning the anti-freezing and anti-drying properties can be found in the Supporting Information.

The schematic diagram of the working principle of AVN-based OHS-TENG is shown in Figure 3a. Based on the triboelectric effect, skin and silicone rubber (SR) are considered as positive and negative triboelectric material, respectively. While the organohydrogel (OH) is used as electrode in this work, the ionic conductive polymer network greatly benefits the ion transport.[35,36] During the continuous contact and separation cycle, the charge balance is obtained at the SR−OH interface and wire−OH interface because the electrons quickly flow from and back to the ground. Thus, alternating current and voltage signals will be generated when AVN-based OHS-TENG is repeatedly contacted and released with skin. Figure 3b is the simulated electrical potential distribution of this device based on the COMSOL Multiphysics, of which the highest potential is generated when skin is fully separated from the device.

The open-circuit voltage (V_{OC}) and short-circuit current density (I_{SC}) were measured for AVN-based OHS-TENGs with different glycerol immersion time from 0 to 5 h. As shown in Figure 3c−e, a longer immersion time resulted in a lower output, as confirmed by the output of 10 devices for each condition. This trend could be attributed to the following two reasons. One is that a longer immersion time causes an excessive overflow of NaCl, leading to a lower conductivity. SI Figure S10 reveals that the conductivity of the original AVN-based hydrogel reached 7.56 × 10^{-4} S/cm and it dropped to 5.93−1.02 × 10^{-5} S/cm with 0.5−5 h glycerol immersion. It is noted that both the conductivity and output gradually tend to be stable when soaking time exceeds 1 h. The other reason is that the solvent replacement caused the inside electrode to shrink, as referred to the inserted photograph of SI Figure S7 and Figure S9. Moreover, the output difference of various devices before and after 1-h glycerol immersion in Figure 3f further proved the conductive charge channel inside the AVN hydrogel system, caused by the coupling effect of sodium/hydrogen bonds and double networks, plays an important role for organohydrogels to be effectively used in TENGs.

The long-term output stability versus running cycles and storage time was also systematically tested. As shown in SI Figure S11a, the V_{OC} of AVN-based device with 1-h glycerol immersion maintained almost the same within 3000 cycles. In SI Figure S11b, the performance of the device without glycerol immersion degraded rapidly as the storage time increased due to its dry-out property; the glycerol-immersed devices maintained stable output after four-month storage in the air. Figure 3g shows the V_{OC} retention and storage time of our

https://doi.org/10.1021/acsnano.1c03830
ACS Nano XXXX, XXX, XXX−XXX

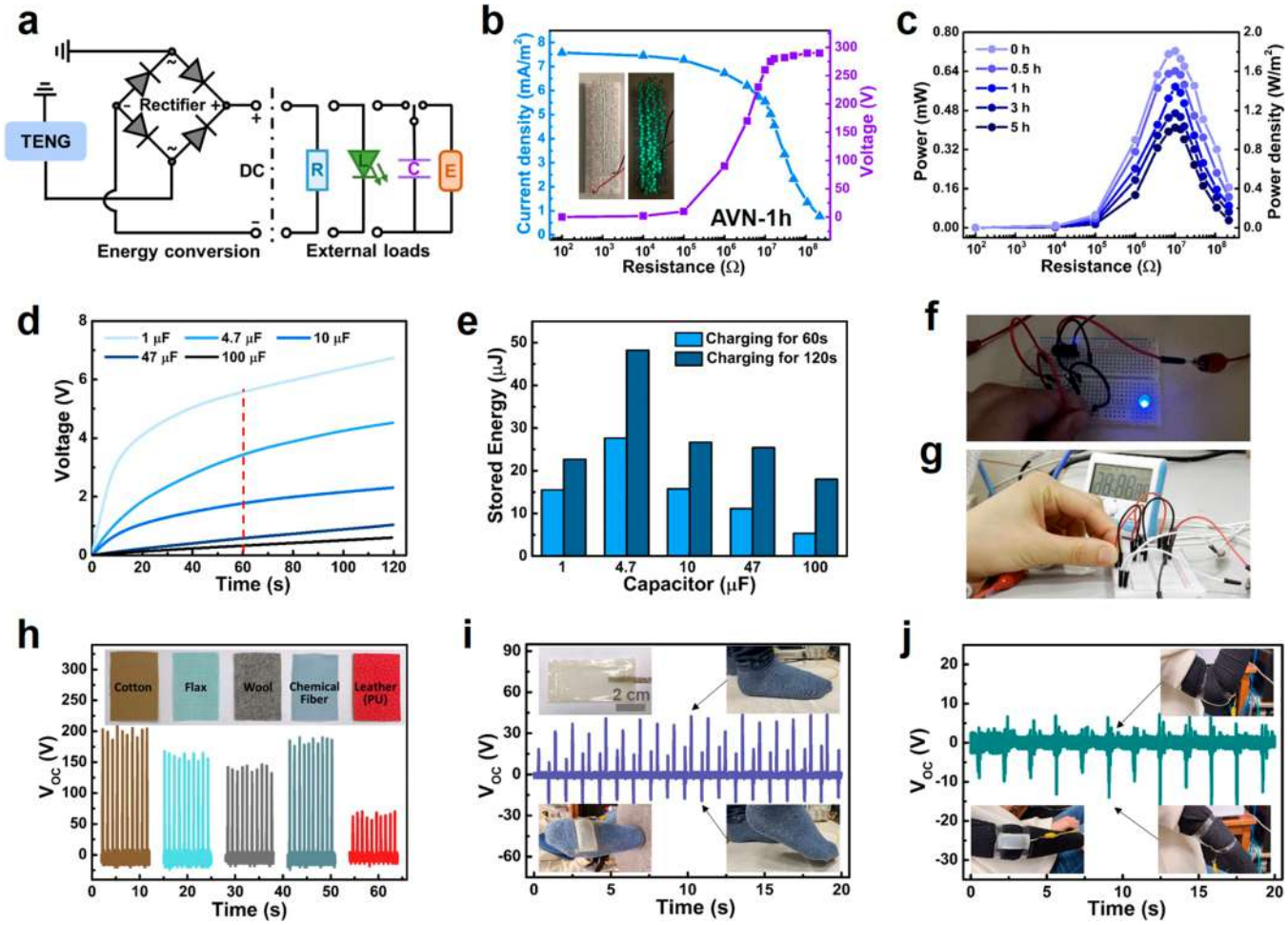

Figure 4. Resistance and capacitance behavior of AVN-based OHS-TENG and its wearable applications: (a) Schematic diagram of the circuit with external loads, (b) dependence of the output voltage and current density in the load resistance range of 100 Ω ~ 220 MΩ, inset is the photograph of 120 LEDs powered by finger tapping, (c) dependence of the power and power density at different glycerol immersion time, (d) charging behavior, and (e) energy stored of the device when connected with different capacitors, (f) a blue LED powered by a 1 μF capacitor after tapping the device for 10 times, (g) the screen of a Timer powered by a 4.7 μF capacitor after tapping the device for 480 times, V_{OC} response to (h) different clothing materials and body motions such as (i) walking and (j) elbow bending.

OHS-TENG as compared with other HS-TENG and OHS-TENG counterparts.[12−15,18,28,31,32,34,37] Most of these reported works can only retain V_{OC} for no more than 30-day storage for HS-TENGs and 60-day storage for OHS-TENGs under ambient condition while the AVN-based device can be retained for four months without degradation.

Considering the anti-freezing and anti-drying properties of the device, the effect of temperature on its output was studied. Unlike the previous works using hot plate/oven and freezer to control the temperature,[12−15] this work designed a real-time temperature-output-monitoring system by connecting a TE module, a power supply and a thermometer, as depicted in SI Figure S12a. This real-time system brings higher accuracy and sensitivity to temperature changes, and thus provides more objective results in terms of temperature effects. It is indicated that the AVN-based device with 1-h glycerol immersion kept almost the same V_{OC} over a wide temperature range of −50−100 °C (SI Figure S12b). As shown in Figure 3h, our work has realized the best temperature tolerance ability and the widest operating temperature window in all existing HS-TENG systems. Moreover, the potential impacts of environmental humidity and sweat on the skin surface on the device output were also studied as shown in SI Figure S13 and the detailed analysis can be found in the Supporting Information.

Figure 4a is the schematic diagram with a rectifier circuit connected with external loads such as LEDs, resistors, capacitors and electronics for demonstrating the real-time applications using AVN-based OHS-TENG. Figure 4b and SI Movie S1 showed that the device can light up 120 green LEDs connected in series by finger tapping. When connected with resistors, the output voltage increased and the current decreased as the load resistance changed from 100 Ω to 220 MΩ (Figure 4b and SI Figure S14). The maximum power density of around 1.02−1.81 W/m^2 can be obtained at a load resistance of 10 MΩ (Figure 4c), which is higher than many reported HS-TENGs and OHS-TENGs as summarized in SI Table S2.[12−15,17,18,28,31,37−40]

Meanwhile, a series of capacitors were used to study the charging behavior of the device. As plotted in Figure 4d, the 1 μF and 4.7 μF capacitors can reach voltages of around 5 and 3 V, respectively, by tapping with fingers in only 60 s. The energy stored of these capacitors at different charging time was further investigated, and it is found that tens μJ energy can be stored into the capacitors with finger tapping for 60−120 s, in which the optimal paired capacitor is 4.7 μF (Figure 4e). As shown in

https://doi.org/10.1021/acsnano.1c03830
ACS Nano XXXX, XXX, XXX−XXX

Figure 4f and SI Movie S2, a 1 μF capacitor was chosen to store energy, and the blue LED can be lighted up by tapping the finger 10 times. In addition, a 4.7 μF capacitor can be used to store the finger tapping energy with 480 times to power on the screen of a Timer (Figure 4g and SI Movie S3).

To further explore the feasibility of wearable applications, five kinds of common clothing materials (including cotton, flax, wool, chemical fiber and PU leather) were worn on the tester's hand with continuously contacted and separated the device. Their corresponding output can be observed in Figure 4h, where 70−200 V of V_{OC} were obtained according to different clothing materials. Although the performance is not as good as the skin, it proves the concept that the device can be attached to various clothes for wearable electronics. Accordingly, an AVN-based OHS-TENG with the electrode of 10 cm^2 was fabricated and attached to the tester's foot with sock and tester's elbow with T-shirt. Each time the tester finished a foot up and down cycle, the output generation process can be clearly measured by the machine (Figure 4i and SI Movie S4). The effective V_{OC} signal change can also be produced by the elbow bending and releasing process (Figure 4j). In addition to tapping and bending, output signals can also be generated by tapping a stretching device or with continuous stretching and releasing cycles as shown in SI Figure S15, indicating the developed device in this work is able to be used at different deformed states in real life and how great potential for human motion energy harvesting in the application of wearable electronics.

CONCLUSION

This work developed a sustainable and stretchable bio-mechanical energy harvester based on ionic conductive organohydrogels. The generated hydrogen bonds and sodium bonds via the Hofmeister effect and electrostatic interaction help the hydrogel to form an effective and stable charge channel, minimizing the conductivity decrease during the glycerol replacement method. Therefore, the device can generate a high peak power density of 1.02−1.81 W/m^2, which can directly light up 120 green LEDs connected in series or charge a capacitor to drive an electronic timer. Moreover, the developed OHS-TENG also shows excellent output stability in terms of storage time (at least 4 months) and temperature (−50−100 °C). Due to its high response sensitivity to different clothing materials, the proof-of-concept wearable OHS-TENGs were showcased for human motion energy harvesting. Besides the excellent performance and stability, the OHS-TENGs have advantages for practical application including a wide operation window, low cost, simple system, and nontoxic. This work provides a versatile platform and understanding for the future development of OHS-TENG with high output performance.

METHODS

Synthesis of Organohydrogel. The AVN hydrogel was synthesized by dissolving poly(vinly alcohol) (PVA, 10 wt %) into the deionized water at 95 °C. Afterward, NaCl (2 M) as the ionic charge carrier, acrylamide (AM, 2 M) as the monomer, N,N-methylenebis(acrylamide) (MBA, 0.06 wt %) as the cross-linker and ammonium persulfate (APS, 1 wt %) as the UV-initiator, were sequentially dissolved in the cooled PVA solution. The weight percentages of PVA, MBA, and APS are with respect to the weight of AM. After degassed, the hydrogel precursor was poured into a PTFE module and illuminated with UV light (365 nm). Following that, the as-prepared hydrogel was immersed in the glycerol solution at room temperature, where the immersion time was varied at 0−5 h. Finally, the surface solvent of the formed organohydrogel was removed by weighing papers. For comparison, PAM, PAM/NaCl and PAM/PVA organohydrogels were prepared with the same procedure.

Fabrication of the OHS-TENG. As shown in SI Figure S4, a typical AVN-based OHS-TENG was fabricated via a simple process similar to our previous works.[41,42] First, the SR precursor (Ecoflex 00−30, base A: base B = 1:1) was poured into a PTFE module with a cuboid ($2 \times 2 \times 0.05$ cm^3) in the center. After curing at 80 °C for 2 h, the obtained SR film ($2.5 \times 2.5 \times 0.1$ cm^2) was immersed in benzophenone (BP, 10 wt %)/ethanol solution and then washed with methanol and dried by N_2. Sequentially, the as-prepared hydrogel precursor was poured into the BP-modified SR holder and followed by UV light illumination. The BP treatment here is to increase the mechanical reliability between SR and hydrogel via formed covalent bonds.[43] The obtained hydrogel-based SR film was immersed in the glycerol at room temperature for 0−5 h. Afterward, two organo-hydrogel-based SR films were attached to each other with a Ag tape inside as a wire and silicone sealant (SELLEYS) was used to seal the device edges. After UV irradiation again, the AVN-based OHS-TENG was fabricated.

Characterization and Measurement. The molecular structure of the samples was studied by a Fourier transform infrared spectrometer (FTIR, IRAffinity-1) at a resolution of 2 cm^{-1} and a Raman spectrometer using a laser wavelength of 633 nm (LabRAM HR, HORIBA). The element analysis of the samples was estimated by the Inductive coupled plasma optical emission spectrometer (ICP-OES, Agilent 720ES). The surface morphology of the hydrogels was performed by a scanning electron microscope (SEM, HITACHI, S-4800). The mechanical properties of the materials were conducted using a microcomputer controlled electronic universal testing machine (CMT6103, MTS) with a stretching speed of 50 mm/min. The transmittance of the samples was confirmed by an ultraviolet and visible spectrophotometer (UV−vis, JENWAY, 6850) in the range of 400−800 cm^{-1}. The electrical potential distribution of the device was simulated by COMSOL Multiphysics 5.5 software via finite-element analysis (FEA). The hydrogel conductivity was evaluated by an impedance analyzer (Princeton Applied Research, VersaSTAT 4). The device output was measured by an oscilloscope (RIGOL DS1054Z) with a high voltage probe (RIGOL PR1050D, 100 MΩ,) and a Keithley source meter (Model 2400) at 1 Hz. All output tests were based on AVN-based OHS-TENG with 1-h glycerol immersion unless otherwise noted.

ASSOCIATED CONTENT

Supporting Information

The Supporting Information is available free of charge at https://pubs.acs.org/doi/10.1021/acsnano.1c03830.

Physical properties (FTIR spectra, SEM images, Raman spectra, ICP-OES data, device photographs, stress−strain curves, and optical transparency), antifreezing and antidrying properties, conductivity and output performance (long-term output stability, temperature, environmental humidity, and skin sweat effects on the output, resistance behavior, and stretching effect on the output), and comparison (PDF)

Movie S1 (MP4)

Movie S2 (MP4)

Movie S3 (MP4)

Movie S4 (MP4)

AUTHOR INFORMATION

Corresponding Authors

Yang Luo − *Department of Physics, City University of Hong Kong, Kowloon, Hong Kong*; Email: yluo24-c@my.cityu.edu.hk

https://doi.org/10.1021/acsnano.1c03830
ACS Nano XXXX, XXX, XXX−XXX

Shien-Ping Feng − *Department of Mechanical Engineering, The University of Hong Kong, Hong Kong;* orcid.org/0000-0002-3941-1363; Email: hpfeng@hku.hk

Authors

Yinghong Wu − *Department of Mechanical Engineering, The University of Hong Kong, Hong Kong*

Jingkui Qu − *National Engineering Laboratory for Hydrometallurgical Cleaner Production Technology, Institute of Process Engineering, Chinese Academy of Sciences, Beijing 100190, China*

Xinghan Zhang − *National Engineering Laboratory for Hydrometallurgical Cleaner Production Technology, Institute of Process Engineering, Chinese Academy of Sciences, Beijing 100190, China*

Kelong AO − *School of Energy and Environment, City University of Hong Kong, Kowloon, Hong Kong;* orcid.org/0000-0003-3685-0915

Zhiwen Zhou − *Department of Mechanical Engineering, The University of Hong Kong, Hong Kong*

Zeyang Zheng − *Department of Mechanical Engineering, The University of Hong Kong, Hong Kong*

Yijie Mu − *Department of Mechanical Engineering, The University of Hong Kong, Hong Kong*

Xinya Wu − *Department of Mechanical Engineering, The University of Hong Kong, Hong Kong*

Complete contact information is available at: https://pubs.acs.org/10.1021/acsnano.1c03830

Notes

The authors declare no competing financial interest.

ACKNOWLEDGMENTS

This work was supported by the General Research Fund of the Research Grants Council of Hong Kong Special Administrative Region, China under Award Nos. 17206519 and 17203520. This work was also partially supported by HKU-Zhejiang Institute of Research and Innovation (HKU-ZIRI), China.

REFERENCES

(1) Zhou, J.; Cheng, J.; Wang, B.; Peng, H.; Lu, J. Flexible Metal-Gas Batteries: A Potential Option for Next-Generation Power Accessories for Wearable Electronics. *Energy Environ. Sci.* **2020**, *13*, 1933−1970.

(2) Song, Y.; Min, J.; Gao, W. Wearable and Implantable Electronics: Moving toward Precision Therapy. *ACS Nano* **2019**, *13*, 12280−12286.

(3) Guo, Y.; Chen, S.; Sun, L.; Yang, L.; Zhang, L.; Lou, J.; You, Z. Degradable and Fully Recyclable Dynamic Thermoset Elastomer for 3D-Printed Wearable Electronics. *Adv. Funct. Mater.* **2021**, *31*, 2009799.

(4) Chen, S.; Huang, T.; Zuo, H.; Qian, S.; Guo, Y.; Sun, L.; Lei, D.; Wu, Q.; Zhu, B.; He, C.; Mo, X.; Jeffries, E.; Yu, H.; You, Z. A Single Integrated 3D-Printing Process Customizes Elastic and Sustainable Triboelectric Nanogerators for Wearable Electronics. *Adv. Funct. Mater.* **2018**, *28*, 1805108.

(5) Graham, S. A.; Dudem, B.; Patnam, H.; Mule, A. R.; Yu, J. S. Integrated Design of Highly Porous Cellulose-Loaded Polymer-Based Triboelectric Films toward Flexible, Humidity-Resistant, and Sustainable Mechanical Energy Harvesters. *ACS Energy Lett.* **2020**, *5*, 2140−2148.

(6) Zohair, M.; Moyer, K.; Eave-Tathert, J.; Meng, C.; Waugh, J.; Print, C. L. Continous Energy Harvesting and Montion Sensing from Flexible Electrochemical Nanogenerators: Toward Smart and Multi-functional Textiles. *ACS Nano* **2020**, *14*, 2308−2315.

(7) Ye, C.; Xu, Q.; Ren, J.; Ling, S. Violin String Inspired Core-Sheath Silk/Steel Yarns for Wearable Triboelectric Nanogeneator Applications. *Adv. Fiber Mater.* **2020**, *2*, 24−33.

(8) Fan, F.; Tian, Z.; Wang, Z. L. Flexible Triboelectric Generator. *Nano Energy* **2012**, *1*, 328−334.

(9) Sun, L.; Huang, H.; Ding, Qi.; Guo, Y.; Sun, W.; Wu, Z.; Qin, M.; Guan, Q.; You, Z. Highly Transparent, Stretchable, and Self-Healable Ionogel for Multifunctional Sensors, Triboelectric Nanogenerator, and Wearable Fibrous Electronics. *Adv. Fiber Mater.* **2021**, DOI: 10.1007/s42765-021-00086-8.

(10) Wang, H. L.; Guo, Z. H.; Pu, X.; Wang, Z. L. Boosting the Power and Lowering the Impedance of Triboelectic Nanogenerators through Manipulating the Permittivity for Wearable Energy Harvesting. *ACS Nano* **2021**, *15*, 7513−7521.

(11) Hua, M.; Wu, S.; Ma, Y.; Zhao, Y.; Chen, Z.; Frenkel, I.; Strzalka, J.; Zhou, H.; Zhu, X.; He, X. Strong Tough Hydrogels *via* the Synergy of Freeze-Casting and Salting Out. *Nature* **2021**, *590*, 594−599.

(12) Pu, X.; Liu, M.; Chen, X.; Sun, J.; Du, C.; Zhang, Y.; Zhai, J.; Hu, W.; Wang, Z. L. Ultrastretchable, Transparent Triboelectric Nanogenerator as Electronic Skin for Biomechanical Energy Harvesting and Tactile Sensing. *Sci. Adv.* **2017**, *3*, No. e1700015.

(13) Wang, Y.; Zhang, L.; Lu, A. Highly Stretchable, Transparent Cellulose/PVA Composite Hydrogel for Multiple Sensing and Triboelectric Nanogenerators. *J. Mater. Chem. A* **2020**, *8*, 13935−13941.

(14) Bao, D.; Wen, Z.; Shi, J.; Xie, L.; Jiang, H.; Jiang, J.; Yang, Y.; Liao, W.; Sun, X. An Anti-Freezing Hydrogel Based Stretchable Triboelectric Nanogenerator for Biomechanical Energy Harvesting at Sub-Zero Temperature. *J. Mater. Chem. A* **2020**, *8*, 13787−13794.

(15) Sun, L.; Chen, S.; Guo, Y.; Song, J.; Zhang, L.; Xiao, L.; Guan, Q.; You, Z. Ionogel-Based, Highly Stretchable, Transparent, Durable Triboelectric Nanogenerators for Energy Harvesting and Motion Sensing over a Wide Temperature Range. *Nano Energy* **2019**, *63*, 103847.

(16) Chen, F.; Zhou, D.; Wang, J.; Li, T.; Zhou, X.; Gan, T.; T-Wang, S.; Zhou, X. Rational Fabrication of Anti-Freezing, Non-Drying Tough Organohydrogels by One-Pot Solvent Displacement. *Angew. Chem., Int. Ed.* **2018**, *57*, 6568−6571.

(17) Huang, L.-B.; Dai, X.; Sun, Z.; Wong, M.-C.; Pang, S.-Y.; Han, J.; Zheng, Q.; Zhao, C.-H.; Kong, J.; Hao, J. Environment-Resisted Flexible High Performance Triboelectric Nanogenerators Based on Ultrafast Self-Healing Non-Drying Conductive Organohydrogel. *Nano Energy* **2021**, *82*, 105724.

(18) Sun, H.; Zhao, Y.; Jiao, S.; Wang, C.; Jia, Y.; Dai, K.; Zheng, G.; Liu, C.; Wan, P.; Shen, C. Environment Tolerant Conductive Nanocomposite Organohydrogels as Flexible Strain Sensors and Power Sources for Sustainble Electronics. *Adv. Funct. Mater.* **2021**, *31*, 2101696.

(19) Wu, S.; Hua, M.; Alsaid, Y.; Du, Y.; Ma, Y.; Zhao, Y.; Lo, C.-Y.; Wang, C.; Wu, D.; Yao, B.; Strzalka, J.; Zhou, H.; Zhu, X.; He, X. Poly(vinyl Alcohol) Hydrogels with Broad-Range Tunable Mechanical Properties *via* the Hofmeister Effect. *Adv. Mater.* **2021**, *33*, 2007829.

(20) Yiming, B.; Han, Y.; Han, Z.; Zhang, X.; Li, Y.; Lian, W.; Zhang, M.; Yin, J.; Sun, T.; Wu, Z.; Li, T.; Fu, J.; Jia, Z.; Qu, S. A Mechanically Robust and Versatile Liquid-Free Ionic Conductive Elastomer. *Adv. Mater.* **2021**, *33*, 20006111.

(21) Li, Z.-F.; Zhu, Y.-C.; Liu, H.-X. Prediction and Characterization of the Single-Electron Sodium Bond Vomplexes Y−C···Na−H[Y = H_3, H_3CH_2, $(H_3C)_2H$ and (H_3C)]. *Phys. Chem. Chem. Phys.* **2009**, *11*, 11113−11120.

(22) Wu, J.; Wu, Z.; Xu, H.; Wu, Q.; Liu, C.; Yang, B.-R.; Gui, X.; Xie, X.; Tao, K.; Shen, Y.; Miao, J.; Norford, L. K. An Intrinsically Stretchable Humidity Sensor Based on Anti-Drying, Self-Healing and Transparent Organohydrogels. *Mater. Horiz.* **2019**, *6*, 595−603.

(23) Wu, J.; Wu, Z.; Lu, X.; Han, S.; Yang, B.-R.; Gui, X.; Tao, K.; Miao, J.; Liu, C. Ultrastretchable and Stable Strain Sensors Based on

Antifreezing and Self-Healing Ionic Organohydrogels for Human Motion. *ACS Appl. Mater. Interfaces* **2019**, *11*, 9405−0414.
(24) Wu, J.; Wu, Z.; Huang, W.; Yang, X.; Liang, Y.; Tao, K.; Yang, B.-R.; Shi, W.; Xie, X. Stretchable, Stable, and Rom-Temperature Gas Sensors Based on Self-Healing and Transparent Organohydrogels. *ACS Appl. Mater. Interfaces* **2020**, *12*, 52070−52081.
(25) Wu, Z.; Yang, X.; Wu, J. Conductive Hydrogel- and Organohydrogel-Based Stretchable Sensors. *ACS Appl. Mater. Interfaces* **2021**, *13*, 2128−2144.
(26) Wei, J.; Wei, G.; Shang, Y.; Zhou, J.; Wu, C.; Wang, Q. Dissolution−Crystallization Transition within a Polymer Hydrogel for a Processable Ultratough Electrolyte. *Adv. Mater.* **2019**, *31*, 1900248.
(27) Chen, G.; Huang, J.; Gu, J.; Peng, S.; Xiang, X.; Chen, K.; Yang, X.; Guan, L.; Jiang, X.; Hou, L. Highly Tough Supramolecular Double Network Hydrogel Electrolytes for an Artificial Flexible and Low-Temperature Tolerant Sensor. *J. Mater. Chem. A* **2020**, *8*, 6776−6784.
(28) Liu, T.; Liu, M.; Dou, S.; Sun, J.; Cong, Z.; Jiang, C.; Du, C.; Pu, X.; Hu, W.; Wang, Z. L. Triboelectric-Nanogenerator-Based Soft Energy-Harvesting Skin Enabled by Toughly Bonded Elastomer/Hydrogel Hybrids. *ACS Nano* **2018**, *12*, 2818−2826.
(29) Song, J.; Chen, S.; Sun, L.; Guo, Y.; Zhang, L.; Wang, S.; Xuan, H.; Guan, Q.; You, Z. Mechanically and Electronically Robust Transparent Organohydrogel Fibers. *Adv. Mater.* **2020**, *32*, 1906994.
(30) Xu, S.; Vogt, D. M.; Hsu, W.-H.; Osborne, J.; Walsh, T.; Foster, J. R.; Sullivan, S. K.; Smith, V. C.; Rousing, A. W.; Goldfield, E. C.; Wood, R. J. Biocompatible Soft Fluidic Strain and Force Sensors for Wearable Devices. *Adv. Funct. Mater.* **2019**, *29*, 1807058.
(31) Lee, Y.; Cha, S. H.; Kim, Y.-W.; Choi, D.; Sun, J.-Y. Transparent and Attachable Ionic Communicators Based on Self-Cleanable Triboelectric Nanogenerators. *Nat. Commun.* **2018**, *9*, 1804.
(32) Wang, L.; Daoud, W. A. Hybrid Conductive Hydrogels for Washable Human Motion Energy Harvester and Self-Powered Temperature-Stress Dual Sensor. *Nano Energy* **2019**, *66*, 104080.
(33) Gao, G.; Yang, F.; Zhou, F.; He, J.; Lu, W.; Xiao, P.; Yan, H.; Pan, C.; Chen, T.; Wang, Z. L. Bioinspired Self-Healing Human-Machine Interactive Touch Pad with Pressure-Sensitive Adhesiveness on Targeted Substrates. *Adv. Mater.* **2020**, *32*, 2004290.
(34) Jing, X.; Li, H.; Mi, H.-Y.; Feng, P.-Y.; Tao, X.; Liu, Y.; Liu, C.; Shen, C. Enhancing the Performance of a Stretchable and Transparent Triboelectric Nanogenerator by Optimizing the Hydrogel Ionic Electrode Property. *ACS Appl. Mater. Interfaces* **2020**, *12*, 23474−23483.
(35) Li, H.; Han, C.; Huang, Y.; Huang, Y.; Zhu, M.; Pei, Z.; Xue, Q.; Wang, Z.; Liu, Z.; Tang, Z.; Wang, Y.; Kang, F.; Li, B.; Zhi, C. An Extremely Safe and Wearable Solid-State Zinc Ion Battery Based on a Hierarchical Structured Polymer Electrolyte. *Energy Environ. Sci.* **2018**, *11*, 941−951.
(36) Mo, F.; Chen, Z.; Liang, G.; Wang, D.; Zhao, Y.; Li, H.; Dong, B.; Zhi, C. Zwitterionic Sulfobetaine Hydrogel Electrolyte Building Separated Positive/Negative Ion Migration Channels for Aqueous Zn-MnO_2 Batteries with Superior Rate Capabilities. *Adv. Energy Mater.* **2020**, *10*, 2000035.
(37) Lai, Y.-C.; Wu, H.-M.; Lin, H.-C.; Chang, C.-L.; Chou, H.-H.; Hsiao, Y.-C.; Wu, Y.-C. Entirely, Intrinsically, and Autonomously Self-Healable, Highly Transparent, and Superstretchable Triboelectric Nanogenerator for Personal Power Sources and Self-Powered Electronic Skins. *Adv. Funct. Mater.* **2019**, *29*, 1904626.
(38) Xu, W.; Huang, L.-B.; Wong, M.-C.; Chen, L.; Bai, G.; Hao, J. Environmentally Friendly Hydrogel-Based Triboelectric Nanogenerators for Versatile Energy Harvesting and Self-Powered Sensors. *Adv. Energy Mater.* **2017**, *7*, 1601529.
(39) Chen, T.; Shi, Q.; Zhu, M.; He, T.; Sun, L.; Yang, L.; Lee, C. Triboelectric Self-Powered Wearable Flexible Patch as 3D Motion Control Interface for Robotic Manipulator. *ACS Nano* **2018**, *12*, 11561−11571.
(40) Sun, H.; Zhao, Y.; Wang, C.; Zhou, K.; Yan, C.; Zheng, G.; Huang, J.; Dai, K.; Liu, C.; Shen, C. Ultra-Stretchable, Durable and Conductive Hydrogel with Hybrid Double Network as High Performance Strain Sensor and Stretchable Triboelectric Nanogenerator. *Nano Energy* **2020**, *76*, 105035.
(41) Wu, Y.; Luo, Y.; Qu, J.; Daoud, W. A.; Qi, T. Liquid Single-Electrode Triboelectric Nanogenerator Based on Graphene Oxide Dispersion for Wearable Electronics. *Nano Energy* **2019**, *64*, 103948.
(42) Wu, Y.; Luo, Y.; Qu, J.; Daoud, W. A.; Qi, T. Sustainable and Shape-Adaptable Liquid Single-Electrode Triboelectric Nanogenerator for Biomechanical Energy Harvesting. *Nano Energy* **2020**, *75*, 105027.
(43) Yuk, H.; Zhang, T.; Parada, G. A.; Loi, X.; Zhao, X. Skin-Inspired Hydrogel-Elastomer Hybrids with Robust Interfaces and Functional Microstructures. *Nat. Commun.* **2016**, *7*, 12028.

https://doi.org/10.1021/acsnano.1c03830
ACS Nano XXXX, XXX, XXX−XXX